Report on Research Project

Topic- Dual-Transformer-Based Asymmetrical Triple-Port Active Bridge (DT-ATAB) Isolated DC–DC Converter

Guided by-Indrajit Sarkar
Department of Electrical Engg

Done by: Amandeep Behera
Roll no:121EE0311

Abstract-In this report, a dual-transformer-based asymmetrical triple-port active bridge converter (DT-ATAB) is proposed to interface two different dc-sources and a load. DT-ATAB consists of three active power electronic converters and two high-frequency transformers. All switches of these converters can be turned on with zero-voltage switching to reduce the switching losses. The bidirectional power flow operation is possible between the ports. The DT-ATAB also reduces the circulating powers between the ports for well-matched transformer turns ratios as compared to those in the other existing triple-port active bridge converters (TAB). Furthermore, the magnetic short-circuit conditions arising in the three-winding transformer of the TAB are mitigated in DT-ATAB. The principle of operation, steady-state analysis, various modes of operation (three-port and two-port modes) are presented. The theoretical analysis of this paper is verified using simulation studies. The illustrated results show that DT-ATAB can be used as a promising multiport converter to interface the multiple sources and load to achieve wide-ranging outputs with the minimal losses.

INTRODUCTION:

The increasing demand for versatile energy management systems capable of integrating conventional, renewable, and storage-based energy sources has necessitated advancements in power electronic converters. Multiport power electronic converters (MPCs) have emerged as a solution for hybrid vehicles, renewable energy generation, microgrids, and uninterruptible power supplies.

MPCs are broadly classified into three types: **nonisolated**, **partially isolated**, and **isolated**. Among these, isolated MPCs stand out due to their ability to provide soft-switching, bidirectional power flow, and voltage isolation. Among isolated MPCs, **Triple-Port Active Bridge (TAB)** converters are prominent. However, TAB converters face significant challenges, such as high circulating power losses, limited phase delay ranges, and magnetic short-circuiting issues in their three-winding transformers.

To address these limitations, this study proposes the **Dual-Transformer-Based Asymmetrical Triple-Port Active Bridge (DT-ATAB)** converter. By employing two high-frequency transformers and enhanced switching techniques, DT-ATAB ensures efficient bidirectional power flow while reducing losses and improving isolation. The study focuses on the operational principles, steady-state analysis, and control strategies for the DT-ATAB, presenting it as a superior alternative to existing MPC designs.

LITERATURE REVIEW:

Existing Multiport Power Converters:

TAB(Triple Active Bridge Converter):

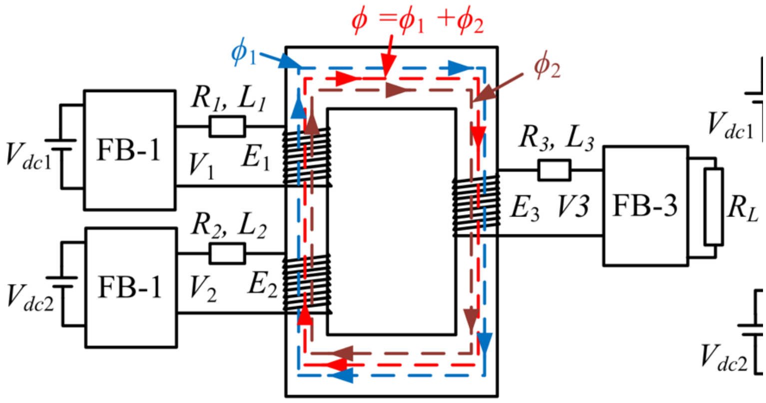

Problems with the existing converter:

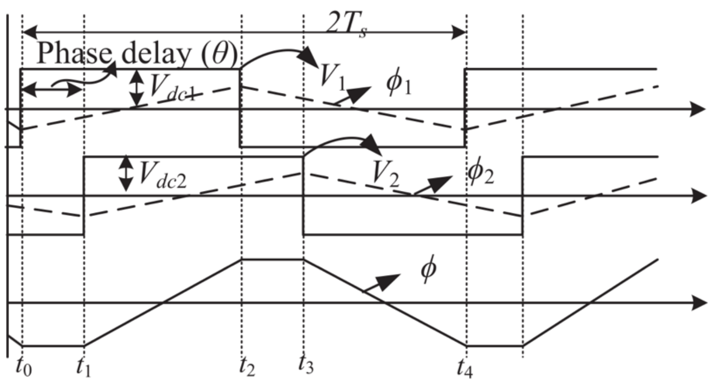

ports -1 and -2 are connected with two different dc sources Vdc1 and Vdc2. In the figure, Rx and Lx represent the leakage impedance of the *xth* transformer winding. The outputs of port-1 and port-2 full bridge converter (FBs)(V1 and V2) generate the fluxes φ1 and φ2, respectively, in the transformer core. The resultant flux (φ) in the core is the summation of these fluxes. The waveforms of V1, V2, φ1, φ2, and φ are shown in Fig. 2. In Fig. 2, θ denotes the phase difference between V1 and V2. It can be seen from Fig. 2 that the polarities of V1 and V2 are positive in the intervals (t1, t2) and negative in the interval (t3, t4). Therefore, φ have positive and negative slopes in (t1, t2) and (t3, t4), respectively. The polarities of V1and V2 are opposite to each other in the intervals (t0, t1) and (t2, t3). Therefore, the slope of φ decreases in these intervals. By neglecting the voltage drops across the leakage impedances, the expression for φ at any instant *t* can be expressed as

$$\phi(t) = \phi(0) + \left[\frac{1}{N_1}\int_0^t V_1\,dt + \frac{1}{N_2}\int_0^t V_2\,dt\right]. \qquad (1)$$

For $t_0 < t < t_1$, (1) can be expressed as:

$$\phi(t) = \phi(t_0) + \left[\frac{1}{N_1}\int_{t_0}^{t} V_{dc1}\,dt + \frac{1}{N_2}\int_{t_0}^{t} (-V_{dc2})\,dt\right]. \quad (2)$$

It can be depicted from (2) that the rate of change in φ decreases in the interval (t0, t1) as shown in Fig. 2. It results in reduced induced voltages or back EMFs (electromotive forces) (E1, E2, and E3) of the transformer. Therefore, the transformer windings connected to source port converters will draw high currents and these currents increase with the increase of phase delay between V1 and V2 resulting in the increased transformer and on-state switching losses. If N1 = N2 = N and Vdc1 =Vdc2 = Vdc, then φ will be constant in the intervals (t1, t2) and(t3, t4) [from (2)]. In such cases, the induced EMFs become zero (as E=−N dφ/dt). Therefore, the transformer windings are magnetically short-circuited (E1 = E2 = E3 = 0) thereby high inrush currents flow from the dc voltage sources. The veracity of this fact is verified using simulation results (see Fig. 11). Therefore, the port-1 and port-2 FBs should be operated to give minimal phase difference between V1 and V2, which reduces the range of output voltages and powers. Additionally, the ports of TAB cannot be isolated by applying turn-on or turn-off gate signals as the windings are connected to the common core and the antiparallel diodes of switches can form the conduction paths.

Summary:

1. Circulating Power Losses due to variation of phase or magnitude of windings voltages which lead to increased copper and core losses, reducing overall efficiency.
2. Magnetic Short-Circuiting Issues**:** causes High inrush current as discussed above.
3. Limited Flexibility in Phase-Shift Control causing narrow range voltage and power flow.
4. Challenges in Source Isolation as the back flow can't be prevented.
5. Load Sharing Imbalance as small mismatch in voltage cause high circulating current.

Operation of DT-ATAB:

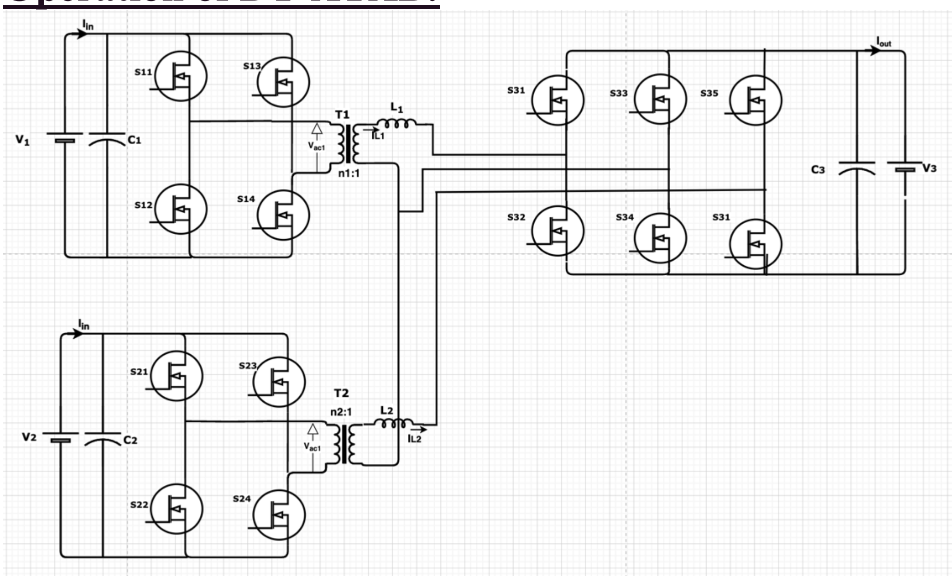

Design Components:
Two full-bridge (FB) converters, one three-leg converter, and two high-frequency transformers.

Principle of Operation:
DT-ATAB can be operated in two different modes of operations: two-port and three-port. In the two-port mode, one port is completely isolated from the system and the remaining two ports are used for the power transfer operation. In the three-port mode, port-1 and port-2 of the DT-ATAB converter are connected to two different dc sources and a load is connected to the port-3 terminal. In this mode of operation, the load power is supplied from both sources simultaneously.

1) Two-Port Mode: In this mode, any one of the source ports of DT-ATAB is active and other source port is isolated from the process by applying turn-on and turn-off gate signals to some of the selected switches as shown in Table I.

TABLE I
TWO-PORT MODE OF OPERATION

Active ports	Switching conditions
Ports-1 and -3	$S_{21}, S_{22}, S_{23}, S_{24}, S_{35}$, and S_{36} are OFF
Ports-2 and -3	$S_{11}, S_{12}, S_{13}, S_{14}, S_{31}$, and S_{32} are OFF

In the two-port mode of operation, the DT-ATAB operates
as a DAB and the expressions of the output power can be expressed as

$$P_{xy} = \frac{1}{2f_s L_{xy}} V_x N V_o D_{xy} \left(1 - D_{xy}\right)$$

where *x* is the input port, *y* is the output port, Vx is the input voltage, Vo is the output voltage, Dxy is the phase-shift ratio, fs is the switching frequency, and Lxy is the equivalent inductance between the ac voltages of the port -*x* and the output port converters.
2) Three-Port Mode: The DT-ATAB is supposed to operate primarily in the three-port mode of operation where all the ports are active. In this paper, two different sources are connected to the ports-1 and -2 to supply the power to a load connected to the port -3 output.

Steady-State Analysis:
The steady-state waveforms of the DT-ATAB converter are illustrated in Fig. 5, and the operation over a complete switching cycle is explained using six time intervals. The corresponding equivalent circuits of the DT-ATAB showing the conduction states of switches and the closed-loop paths for transformer winding currents are depicted in Fig. 6.

Before starting each interval, the secondary currents is1and is2 have negative values. The switches S12,S13,S22,S23,S32,S33,S36 are **ON**, while all other switches are turned **OFF**.

Interval 1 [t0−t1]

This period begins when S12 and S13 are turned OFF and the voltage vA1A2 (or vs1) changes its polarity from negative to positive. The current path for ip1 shifts from S12 and S13 to D11 and D14 naturally. Here, D11 and D14 represent the antiparallel diodes across S11 and S14, respectively. These switches get turn ON after is1 (or ip1) becomes zero (denoted with t10 in Fig. 5) at zero voltage leading to zero-voltage switching. The closed-loop paths for the primary and secondary winding currents during this period are shown in Fig. 6(a). The secondary winding currents during this period can be expressed as

$$i_{s1}\left(t\right) = \left(\frac{NV_{\mathrm{dc}1}+V_o}{L_{f1}}\right)\left(t-t_0\right)+i_{s1}\left(t_0\right)$$

$$i_{s2}\left(t\right) = \left(\frac{-NV_{\mathrm{dc}2}+V_o}{L_{f2}}\right)\left(t-t_0\right)+i_{s2}\left(t_0\right).$$

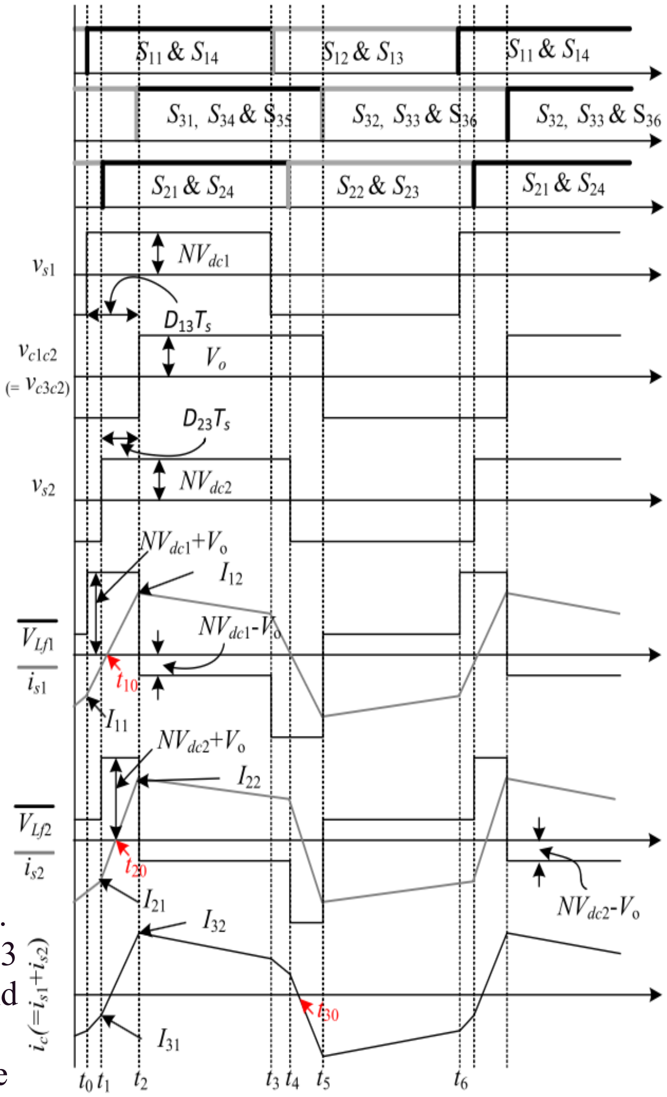

Fig. 5. Steady-state waveforms of DT-ATAB Converter.

Interval-2 [t1− t2]:

[*see* Fig. 6(b)]*:* This period begins when S22 and S23 are turned OFF and the voltage vB1B2 (or vs2) shifts from negative to positive. The current path for ip2 shifts from S22 and S23 to D21 and D24 naturally. The switches S21 and S24 gets turn ON after is2 becomes zero (denoted with t20 in Fig. 5) at zero voltage. The closed-loop paths for the primary and secondary winding currents during this period are shown in Fig. 6(b). The expressions for the secondary winding currents during this period can be expressed as

$$i_{s1}\left(t\right) = \left(\frac{NV_{\mathrm{dc}1}+V_o}{L_{f1}}\right)\left(t-t_0\right)+i_{s1}\left(t_0\right)$$

$$i_{s2}\left(t\right) = \left(\frac{NV_{\mathrm{dc}2}+V_o}{L_{f2}}\right)\left(t-t_1\right)+i_{s2}\left(t_1\right).$$

Interval-3 [t2− t3] [*see* Fig. 6(c)]*:* This period begins when S32, S33, and S36 are turned OFF and the voltages V_{C1C2} and V_{C3C2} shift from negative to positive. The current path for is1 shifts from S32 and S33 to D31 and D34 and that for is2 shifts from S36 and S33 to D35 and D34 naturally. The switches S31,S34, and S35 get turn ON after the currents is1 and is2 become zero (denoted with t30 in Fig. 5) at zero voltage. The closed-loop paths for the primary and secondary winding currents during this period are shown in Fig. 6(c). The expressions for the secondary winding currents during this period can be expressed as

$$\left.\begin{aligned} i_{s1}(t) &= \left(\frac{NV_{dc1}-V_o}{L_{f1}}\right)(t-t_2)+i_{s1}(t_2) \\ i_{s2}(t) &= \left(\frac{NV_{dc2}-V_o}{L_{f2}}\right)(t-t_2)+i_{s2}(t_2) \end{aligned}\right\}.$$

In the similar way as discussed above, the remaining intervals, viz., Interval-4 [t3− t4], Interval-5 [t4− t5], and Interval-6 [t5− t6] can be explained with the help of waveforms shown in Fig. 5 and the equivalent circuits shown in Fig. 6(d), (f).

Output Power and Voltage:

The average currents supplied by the dc sources at port-1 and port-2 can be derived by solving (4)–(6) and applying volt-second balance principle as

$$\bar{I}_1 = \frac{N}{2f_sL_{f1}}D_{13}(1-D_{13}) \text{ and } \bar{I}_2 = \frac{N}{2f_sL_{f2}}D_{23}(1-D_{23}). \quad (7)$$

The powers supplied by both the sources (P1 =Vdc1Idc1andP2 = Vdc2Idc2) can be expressed as:

$$P_1 = \frac{NV_{dc1}V_o}{2f_sL_{f1}}D_{13}(1-D_{13})$$

$$P_2 = \frac{NV_{dc2}V_o}{2f_sL_{f2}}D_{23}(1-D_{23}).$$

By neglecting the switching and transformer losses, the power supplied by both the sources at the output port can beexpressed as

$$\begin{aligned} P_o &= P_1 + P_2 \\ &= \frac{NV_o}{2f_s}\left[\frac{V_{dc1}D_{13}(1-D_{13})}{L_{f1}} + \frac{V_{dc2}D_{23}(1-D_{23})}{L_{f2}}\right] \end{aligned}$$

If a resistance of RL is connected across the output of DT-ATAB, then the power consumed at the output will be equal to V_o^2/R_L . By substituting this value in (9), the expression for the output voltage can be obtained as

$$V_o = \frac{NR_L}{2f_s}\left[\frac{V_{dc1}D_{13}(1-D_{13})}{L_{f1}} + \frac{V_{dc2}D_{23}(1-D_{23})}{L_{f2}}\right]$$

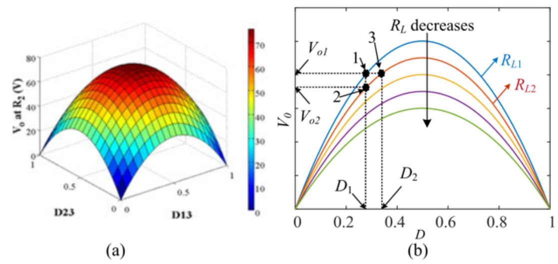

Fig. 7. (a) Variation of the output voltage w.r.t. phase-shift ratios (b) Variation of the output voltage with respect to the phase-shift ratio for different loads.

Now for Vdc1 =Vdc2 = Vdc, Lf 1 = Lf 2 = Lf , and D13 = D23 = D

$$P_o = \frac{NV_oV_{dc}}{f_sL_f}D(1-D) \quad V_o = \frac{NV_{dc}}{f_sL_f}D(1-D)R_L$$

The variation of V_o given in the fig.7.

SIMULATION STUDIES:

Circuit Connection:

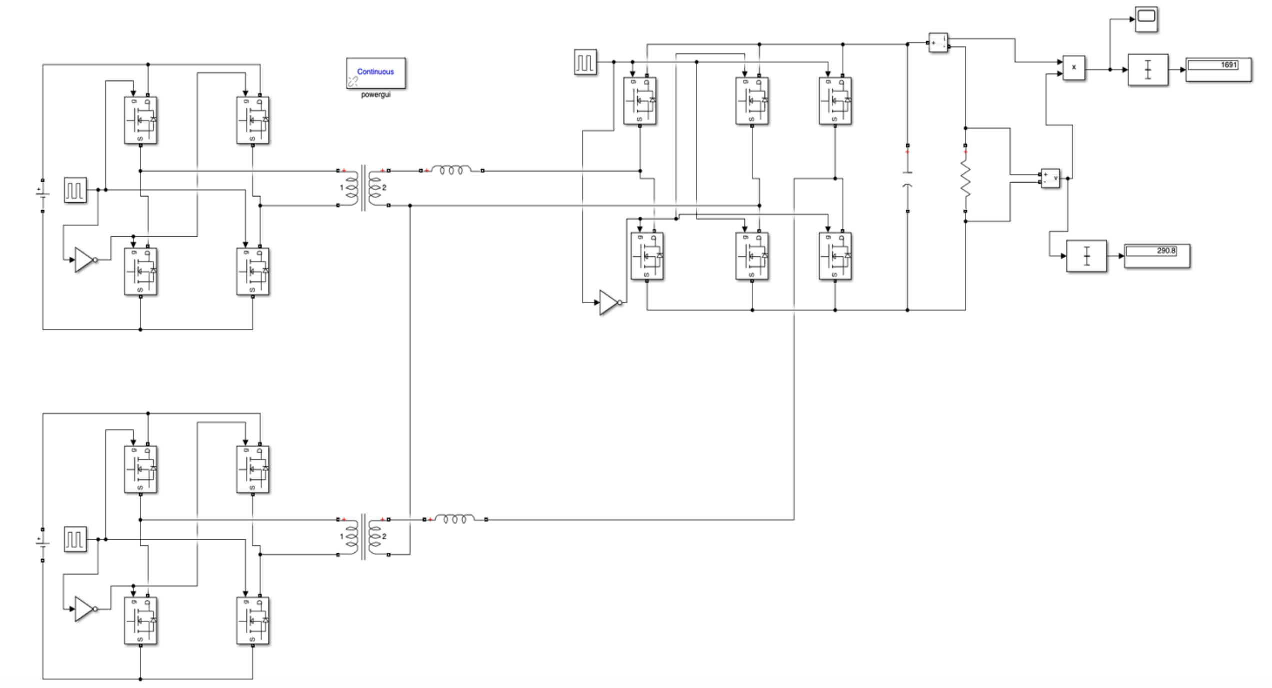

Waveforms:

1. 2-port mode: port-1 and 3 active and port-2 deactivated with D_{13}=.2.

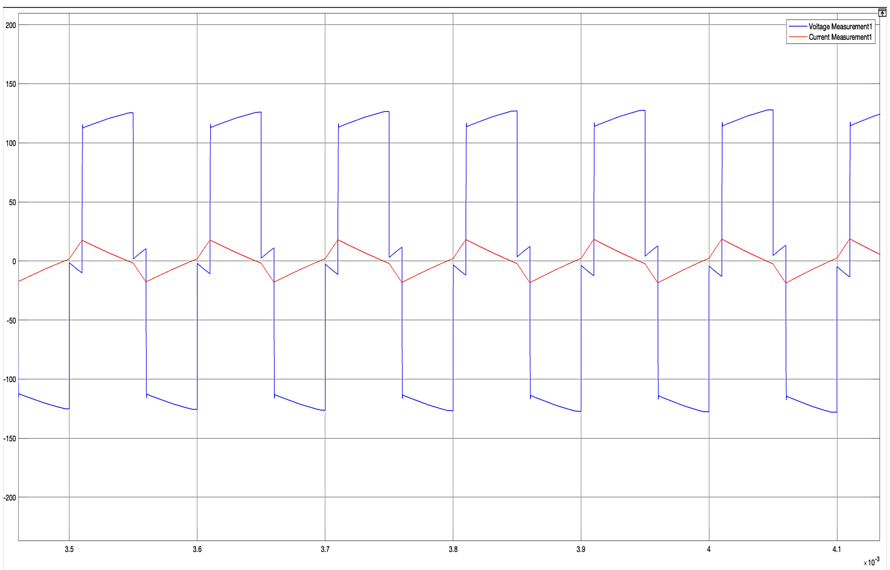

Transformer sec Vs_1 and Is_1

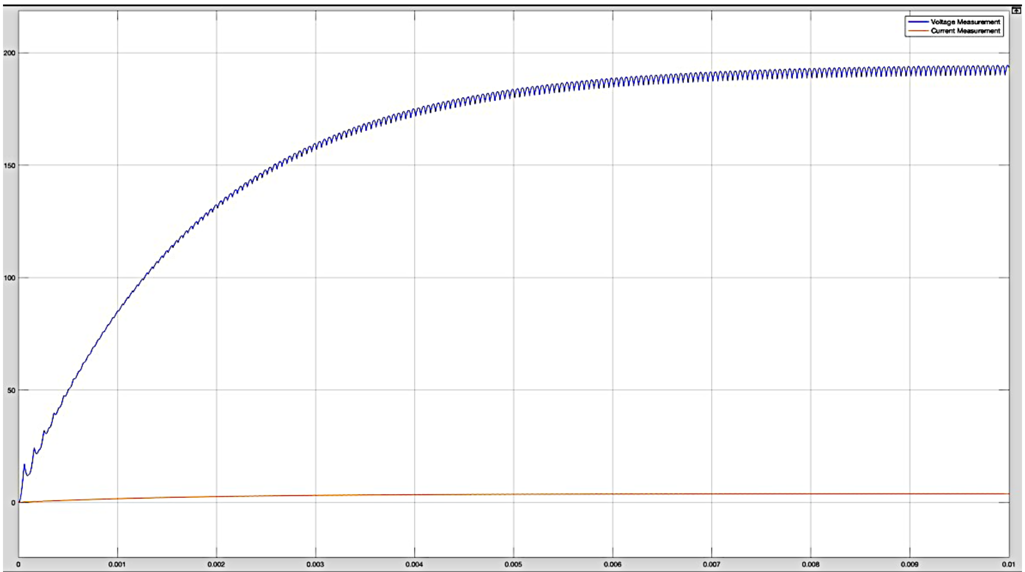

Output Vo and Io

2.3-port mode with $D_{13}=D_{23}=.2$

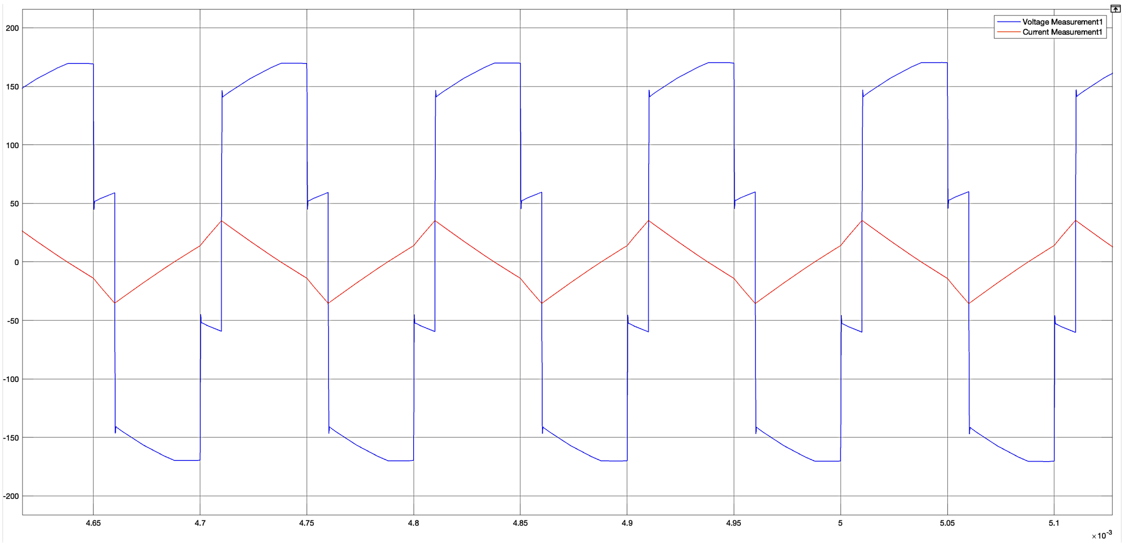

Transformer sec Vs_1 and Is_1

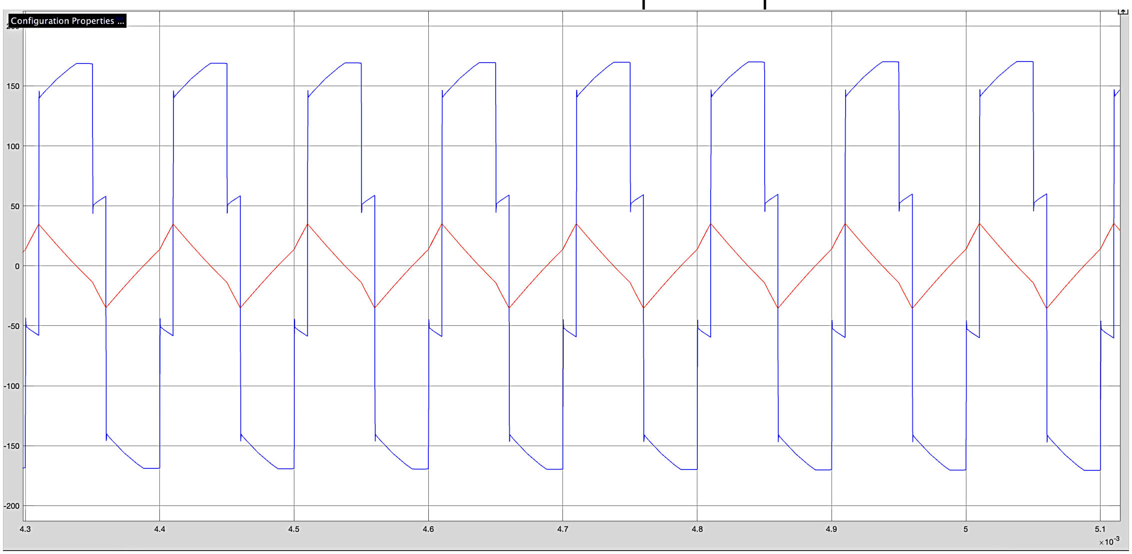

Transformer sec Vs_2 and Is_2

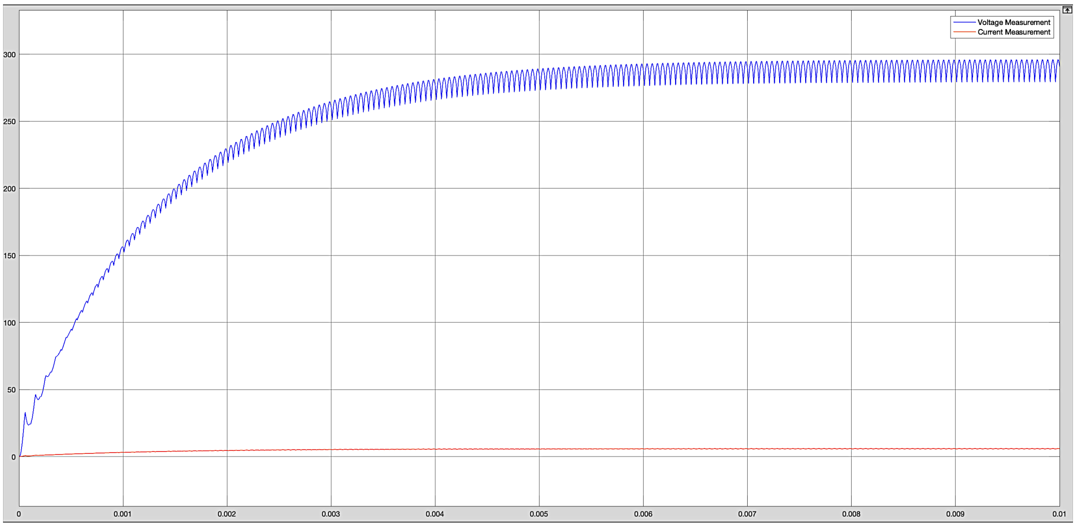

Output V_0 and I_0

<u>3.3-port mode with D_{13}=.2 and D_{23}=.1</u>

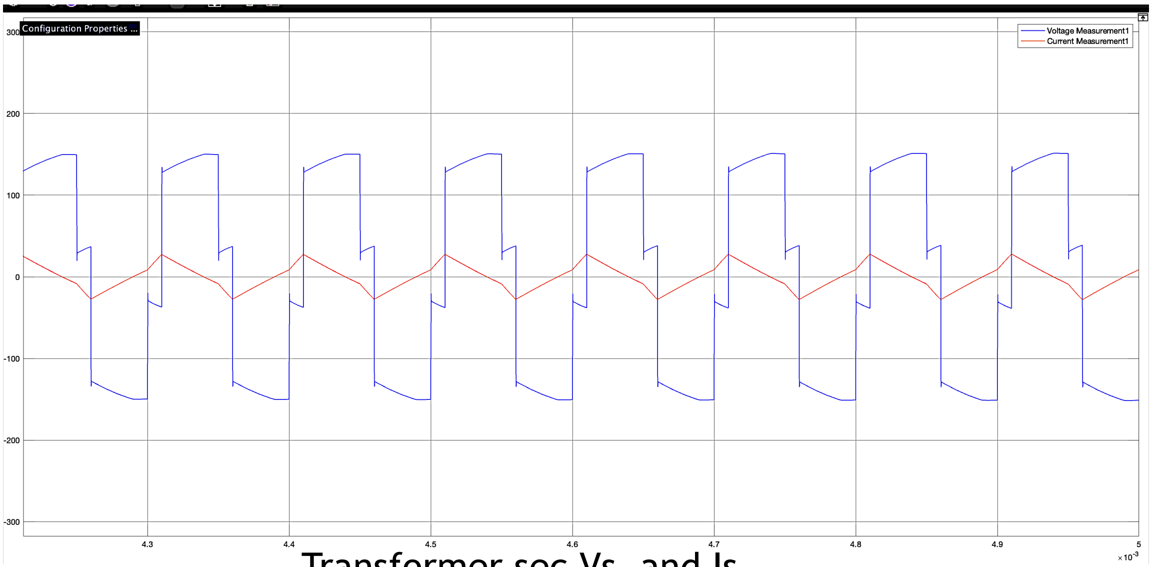

Transformer sec Vs_1 and Is_1

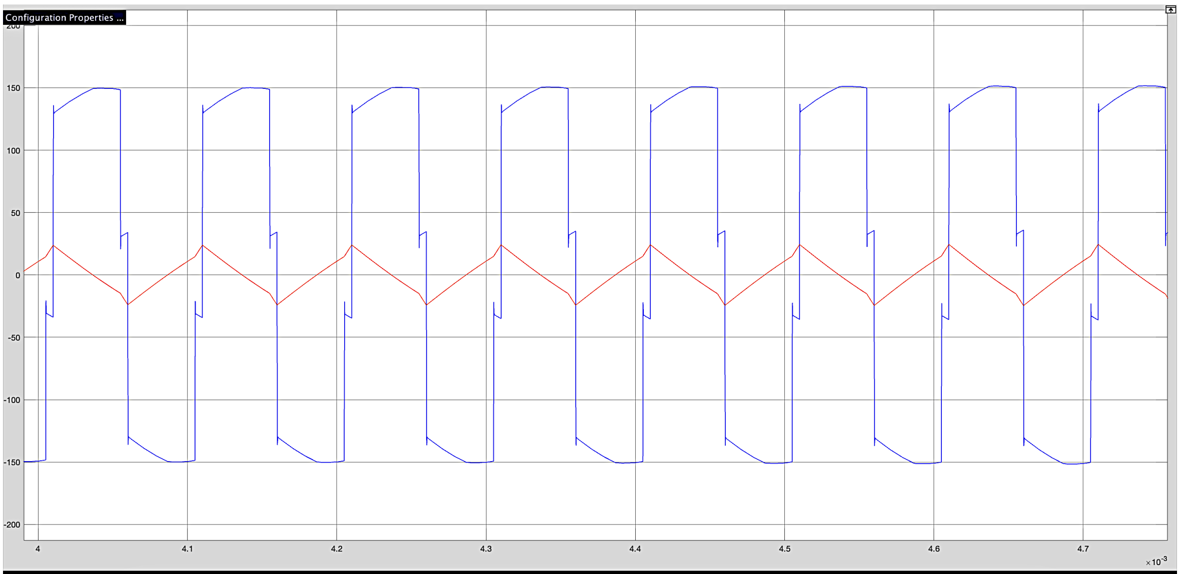

Transformer sec Vs_2 and Is_2

Output voltage with d:

Values of D in %	2port mode	3-port mode
20	74.52	133.9
30	92.67	166.3
40	102	183.3
50	102.7	184.2
60	95.21	170.2
70	79.75	141.5
80	56.88	99.7

FUTURE PLAN OF OPERATION:

1. Simulation of Closed loop control of the converter.
2. Experimental implementation of the converter.

REFERENCE:

Venkat Nag Someswar Rao Jakka, Anshuman Shukla and Georgios D. Demetriades paper on Dual-Transformer-Based Asymmetrical Triple-Port Active Bridge (DT-ATAB) Isolated DC–DC Converter-IEEE TRANSACTIONS ON INDUSTRIAL ELECTRONICS, VOL. 64, NO. 6, JUNE 2017